2022

Modelling and Simulation of the Impact of Soft Faults in a Reversible Air-to-water Propane Heat Pump

Emilio Llopis-Mengual

Emilio Navarro-Peris

Francisco Barcelo-Ruescas

Jose Miguel Corberan

Llopis-Mengual, Emilio; Navarro-Peris, Emilio; Barcelo-Ruescas, Francisco; and Corberan, Jose Miguel, "Modelling and Simulation of the Impact of Soft Faults in a Reversible Air-to-water Propane Heat Pump" (2022). *International Refrigeration and Air Conditioning Conference.* Paper 2335.
https://docs.lib.purdue.edu/iracc/2335

Modeling and simulation of the impact of soft faults in a reversible air-to-water propane heat pump

Belén LLOPIS-MENGUAL[1], Emilio NAVARRO-PERIS[1]*, Francisco BARCELÓ-RUESCAS[1], José M. CORBERÁN[1]

[1]Instituto Universitario de Investigación de Ingeniería Energética (IUIIE),
Universitat Politècnica de València, Camino de Vera s/n, Valencia, 46022, Spain
e-mail: emilio.navarro@iie.upv.es

* Corresponding Author

ABSTRACT

Heat pumps can be affected by faults that are not easily perceived (soft faults) but could increase their energy consumption and move to more severe ones affecting the reliability of the system. The development of fault detection and diagnosis techniques with an experimental approach requires a huge amount of costly and time-consuming data. The analysis of them sometimes is mixed with coupling effects that make the fault identification in real conditions difficult. This work evaluates the influence of some of the most common sources of soft faults (charge, leaks, coil obstruction), including their cross effect. In order to do that, an air-to-water heat pump of 10 kW using propane as refrigerant has been tested, and based on the experimental campaign, a detailed model of it has been built. Finally, the model has been used to evaluate the effect of the different faults in cooling and heating mode, their cross effects on the heat pump performance, and their relative impact on the different system parameters. This constitutes the first step to developing virtual sensors for these kinds of errors which, in the case of using flammable refrigerants, could significantly reduce the cost of the system.

1. INTRODUCTION

In Europe, 36% of CO2 emissions, including indirect emissions, come from buildings (European Comission, 2018). In order to reduce it, heat pumps are a highly considered technology in the European decarbonization routes (Abbasi et al., 2021). Air-to-water heat pumps can very well contribute to this, as they can use energy from the outdoor air to heat water for heating and DHW. If they are reversible, they can also supply cold water for air-conditioning.

There are soft faults in heat pumps that cannot be easily detected since the system operates normally. However, it operates at a lower performance than it should under certain conditions. These faults occur slowly over time, and their detection and diagnosis are not accessible. Some examples of these faults are undercharge or overcharge, outdoor unit fouling, or compressor valve leakage. Therefore, it is essential to develop fault detection and diagnosis techniques for heat pumps in order to be able to perform proper maintenance.

It is difficult to have available data of heat pumps under fault conditions, as it is time-consuming to test these systems with imposed faults experimentally. Therefore, it is helpful to model and simulate these systems under different fault conditions and levels. Previously, some studies were conducted to model these faults (Cheung & Braun, 2013). They developed a vapor compression system model for predicting fault impacts. These have COP prediction with a maximum error of 21%, and although they calculate similar trends to the experimental tests, some variables have significant differences under fault conditions. In order to have information to develop fault detection and diagnosis, Mehrabi and Yuill conducted a study based on a large set of experimentally tested air-source heat pumps with imposed faults to assign generalized effects on system variables in both cooling and heating (Mehrabi & Yuill, 2018).

Currently, there is a concern about detecting these faults when they occur simultaneously. Few studies have covered this. Boahen et al. experimentally study how to detect refrigerant charge and secondary fluid flow rate failures in cooling mode (Boahen et al., 2021). Hu and Yuill analyze the effects of up to quadruple-fault combinations experimentally imposed on an air-source heat pump in cooling mode (Hu & Yuill, 2021). In the case of flammable refrigerants such as propane, detecting leakage of refrigerant charge is of great importance. Currently, sensors to detect this are either expensive or high maintenance and must be frequently replaced. It is also essential to know how the system may behave if this fault occurs simultaneously with others, as this could modify the detection technique.

In this study, we have modeled in IMST-ART software (Corberán et al., 2002) a reversible air-to-water heat pump using propane as a refrigerant, which we have adjusted from an experimental campaign. Using this model, the effect of several potential faults and their cross effects have been analyzed. With this, we can know their influence on the performance of the system and have an indication of their impact on different system variables in such a way that they could be used as a powerful tool for their detection.

2. METHODOLOGY

2.1 Experimental setup

The experimental set-up considered in this study is a reversible air-to-water heat pump operating with refrigerant R290 (propane). The heat pump (see Figure 1) incorporates a Brazed Plate Heat Exchanger (BPHX) that exchanges heat with water, a Finned-tube Heat Exchanger that exchanges heat with air, a rotary compressor, and an electronic expansion valve. This system has a 4-way valve that allows the heat pump to be reversible and work in both cooling and heating mode.

An experimental campaign has been performed to characterize the heat pump fault-free to adjust and validate a model of the heat pump. Thus, 7 tests have been carried out in heating mode with air temperatures between 7 and 12ºC and water outlet temperatures between 25 and 70ºC. In cooling mode, we performed 3 tests with the air temperature at 35ºC and water outlet temperature between 7 and 18ºC. The temperature on the refrigerant side has been measured with T-type thermocouples at the inlet and outlet of the heat exchangers. Besides, RTD PT100 temperature sensors were used to measure the inlet and outlet of the water and the air inlet temperature. Pressure at the suction and discharge of the compressor is measured with absolute pressure transducers Rosemount 3051. From the uncertainty analysis, we obtain a total error of ±0.8K for the T-type thermocouples, ±0.07 ºC for the RTD, and ±0.06 bar for the pressure transducers.

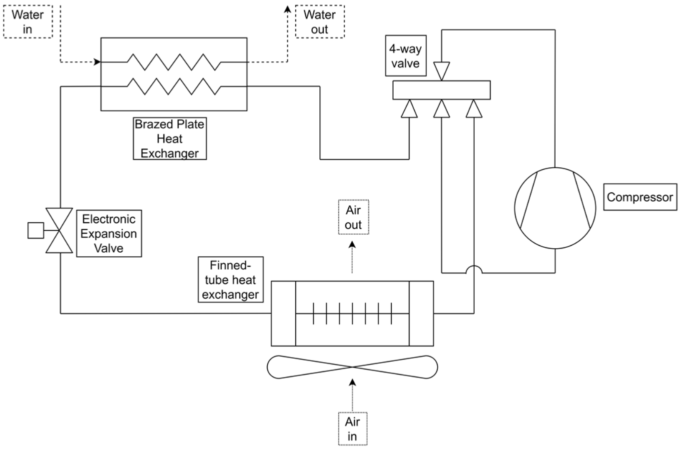

Figure 1: Diagram of the reversible air-to-water propane heat pump.

2.2 Heat pump and soft faults model

The heat pump has been modeled in IMST-ART by incorporating the corresponding data of each submodel. Therefore, we use the geometrical information from the manufacturers' catalogs in the heat exchanger submodels. For the compressor, the capacity and consumption tables for each condition from the manufacturer and their geometrical data has been used. Then, the total system has been simulated under the same conditions in which the experimental campaign was conducted and validate the model by comparing the results with the experimental ones.

The following faults in the model were analyzed: refrigerant undercharge (UC) or overcharge (OC), outdoor unit fouling (OF), and compressor valve leakage (CVL). As IMST-ART uses a detailed model of the heat pump based on physical principles, the results with the imposed faults are expected to be satisfactory. In addition, the same procedure described below has been tested with available data of air-to-air heat pumps with experimentally imposed faults, as

(Kim et al., 2006). The results of the variables they measure and those we obtain are similar, so we assume that they are also comparable with this air-to-water heat pump.
To implement the UC and OC refrigerant fault, IMST-ART can set as input the refrigerant charge of the system. Thus, if we want to introduce UC or OC, we increase or decrease the corrected refrigerant charge by the desired percentage. We refer to the UC or OC fault level as the ratio of the increased (OC) or reduced (UC) charge and the fault-free charge.

The OF fault is caused by an accumulation of dirt and deposits in the heat exchanger, which affects the air-side heat transfer coefficient. In addition, it reduces the airflow by adding a pressure drop in the coil. In this study, we have considered only this second effect, reducing the airflow in the outdoor unit. We have not considered other effects derived from this fault, such as increased fan consumption or changes in the air-side heat transfer coefficient. Therefore, we consider the OF fault level as the percentage of reduced fan airflow with respect to the fault-free fan airflow.

CVL occurs if the compressor's suction or discharge valve does not close properly, and an internal leak occurs, resulting in the mixing of the discharge flow with the suction flow. The effect of this fault is similar to a leak in the 4-way reversible valve. We have simulated this fault in IMST-ART by modifying the compressor submodel so that the refrigerant mass flow rate is reduced with the corresponding fault level, which in the case of CVL, is the ratio of mass flow rate that is bypassed from the discharge to the suction with respect to the mass flow rate of the fault-free refrigerant mass flow rate under the same conditions.

Finally, we have implemented combinations of two of these faults simultaneously in the model to study the cross-effect they may have on the heat pump performance. In addition, we have simulated all these faults in both cooling and heating modes to study the differences that may exist.

3. RESULTS AND DISCUSSION

3.1 Fault-free model validation

The results of comparing the experimental tests and the model simulations under the same conditions are shown in Figure 2. The condenser temperature (Tc) has an RMSE of 1.044 ºC, the evaporator temperature (Te) of 0.917ºC, and the subcooling (SC) of 1.676 K. With this, we can verify that our IMST-ART model correctly reproduces the behavior of the system.

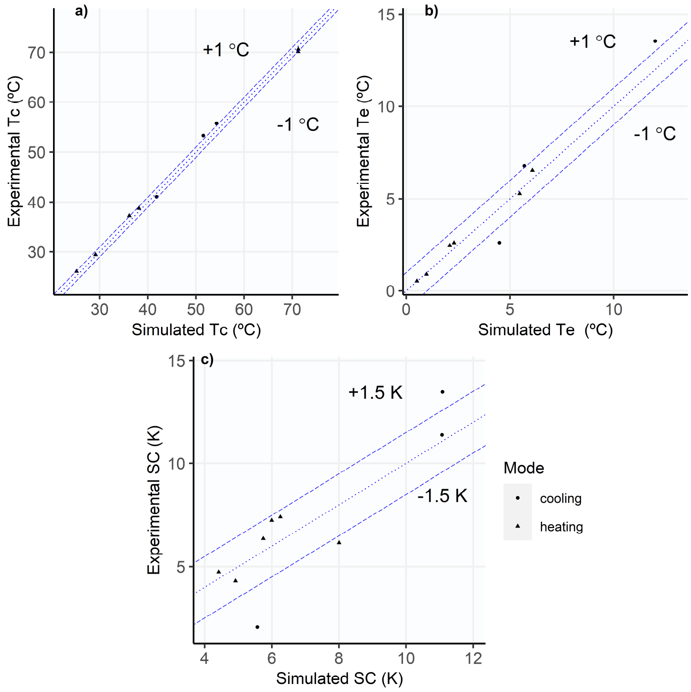

Figure 2: Comparison of the simulated and experimental results in Tc (a), Te (b), and SC (c).

3.2 Single faults

Figures 3, 4, and 5 show the impacts of each of the single faults imposed on the model on Tc, SC, and Te. We have simulated the heat pump in cooling mode at an air inlet temperature of 25ºC and a water outlet at 15ºC (A25W15). For the heating mode, we have considered the air temperature at 7ºC and the water outlet temperature at 70ºC (A7W70).

Regarding UC and OC, it is observed in Figure 3 that as the refrigerant charge increases, Tc increases, and when reducing, it decreases. This behavior is because the refrigerant is concentrated in a liquid state at the condenser outlet. Therefore, by increasing the refrigerant charge, the effective heat transfer area of the condensation process is reduced, which would require more temperature difference between the refrigerant and the hot source to maintain the Tc. As the hot source temperature is constant, Tc increases. For the same reason, in Figure 4, the SC increases when the refrigerant charge increases and decreases when there is UC. In heating mode, the system behaves the same. However, in this case, the condenser is not the finned tube but the BPHX, so it has less internal volume, and the amount of liquid that accumulates at its outlet is lower. Thus, the variations of Tc and SC occur in a smaller amount than in cooling mode for the same variation of refrigerant charge. In addition, this also produces that in the case of Tc (Figure 3b), it changes more with OC than with UC in heating mode. Concerning Te (Figure 5), both in cooling and heating, no changes are observed in the case of UC or OC since we consider that the electronic expansion valve can control the superheat while at the condenser outlet, the refrigerant is in a liquid state (SC>0). Therefore, evaporator temperature and pressure are maintained in these cases regardless of the fault level.

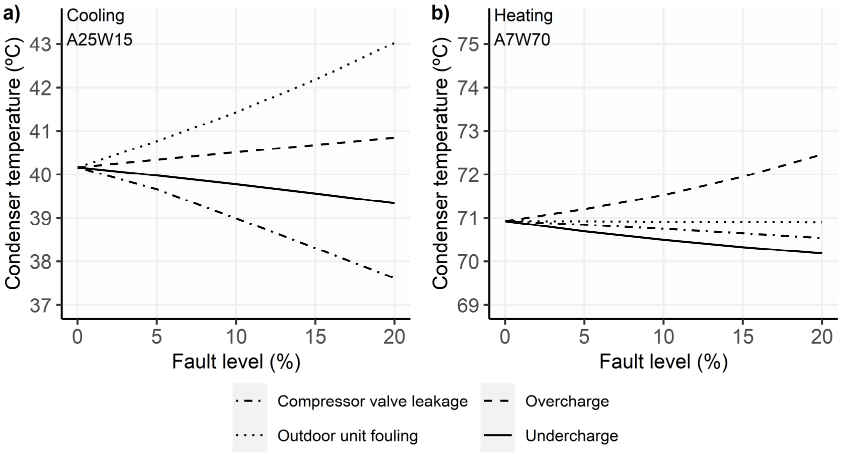

Figure 3: Condenser temperature at different fault levels in cooling (a) and heating mode (b).

For OF fault, the outdoor unit is the condenser in cooling mode. Therefore, according to Figure 3a, as the fault level increases (airflow through the condenser decreases), the condenser heat transfer capacity decreases, and Tc increases. In cooling mode, Te (Figure 5a) is not affected, as OF affects the high-pressure side. In addition, for SC (Figure 4a), as condensing pressure and temperature increase and low-pressure side conditions remain almost constant, SC increases slightly as the fault level increases. Nevertheless, in heating mode, the outdoor unit is the evaporator. Therefore, neither Tc (Figure 3b) nor SC (Figure 4b) is affected in this mode. However, there is a variation in Te (Figure 5b) since a decrease in the air flow rate through the evaporator causes a drop in Te.

In CVL fault, leakage occurs at the discharge, which mixes with the suction flow, thus causing a decrease in pressure at the discharge condition and an increase at the suction condition. Therefore, we can see in Figure 3 that Tc decreases with fault level. In Figure 4, the SC decreases because of discharge pressure and Tc reduction. Figure 5 shows how Te increases with the fault level due to the pressure and temperature increase in the suction conditions. In addition, in Figures 3 and 4, we can see that the system can maintain and reduces less Tc in heating mode than in cooling mode, mainly because in this mode, the condenser is the BPHX, which is more optimized than the coil and. With Te, it is the opposite (Figure 5) since it is in the heating mode where the greatest variation with the fault level is observed, as, in this mode, the coil is the evaporator.

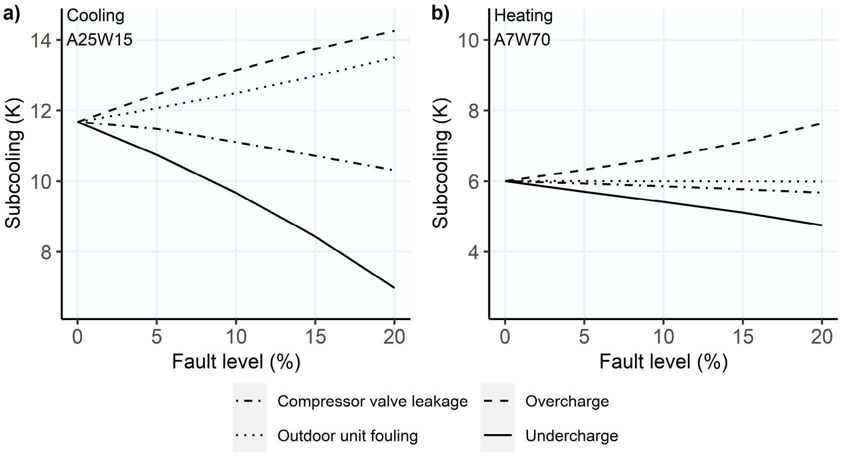

Figure 4: Subcooling at different fault levels in cooling (a) and heating mode (b).

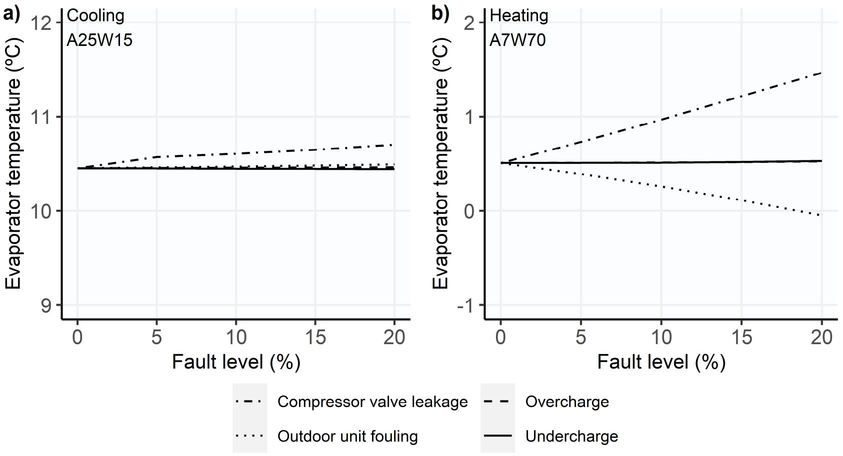

Figure 5: Evaporator temperature at different fault levels in cooling (a) and heating mode (b).

3.3 Simultaneous compressor valve leakage and refrigerant undercharge/overcharge

This section shows the results of simultaneously simulating the CVL and refrigerant UC or OC faults. The conditions under which the simultaneous faults have been simulated are the same as for the single faults, i.e., for cooling, A25W15, and heating, A7W70. To estimate the impact of simultaneous faults on the heat pump, we have obtained the COP as heating or cooling capacity depending on the mode divided by the compressor consumption. We have not considered other consumptions such as fan or pump input power.

Thus, we can observe in Figure 6 that in cooling mode, Tc increases as the refrigerant charge grows and decreases as the CVL fault level increases. Therefore, when a CVL fault occurs up to 5%, if there is 10-20% OC, no changes in Tc are found. That is, one fault overrides another. In the same way, there are areas with the same Tc (e.g., 38.5ºC) in which Tc remains constant at all charge levels if, at the same time, CVL occurs between 5 and 15% of the fault level. This can difficult the task of fault detection and diagnosis of these faults. In heating mode, the system needs less charge (the condenser is the BPHX), and there is less accumulated liquid at the condenser outlet. In the case of UC (refrigerant charge level < 100%), Tc decreases less than it increases with OC (different slope with UC and OC). Also, in cases with OC, CVL fault does not significantly alter Tc's effect. With UC, simultaneous CVL does alter the effects on Tc additionally.

Figure 7 shows the SC in case of simultaneous fault of UC/OC and CVL. Thus, both UC and CVL cause the SC to decrease in cooling mode. Therefore, in the case of UC, having simultaneous CVL does not decrease SC more, with the effect on SC the same as having only UC. In the case of OC coinciding with CVL, it does not cause the SC values to increase as much as if there were only OC (or vice versa, in the case of having high CVL fault level values, if there is OC, the SC does not decrease). In heating mode, as CVL does not have so much impact on the SC in this mode, the system behaves practically the same as with UC/OC even if there is CVL simultaneously.

In Figure 8, we can see the COP result in case of having these simultaneous faults. Thus, we have the optimum for the cooling mode without CVL failure and charge around 100%; moving from that point, the COP worsens. However, in heating mode, the optimum is found for charge values of 100% and lower because it needs less refrigerant charge in this mode. Thus, with OC it worsens more, and by increasing CVL fault level, it worsens less than in cooling mode.

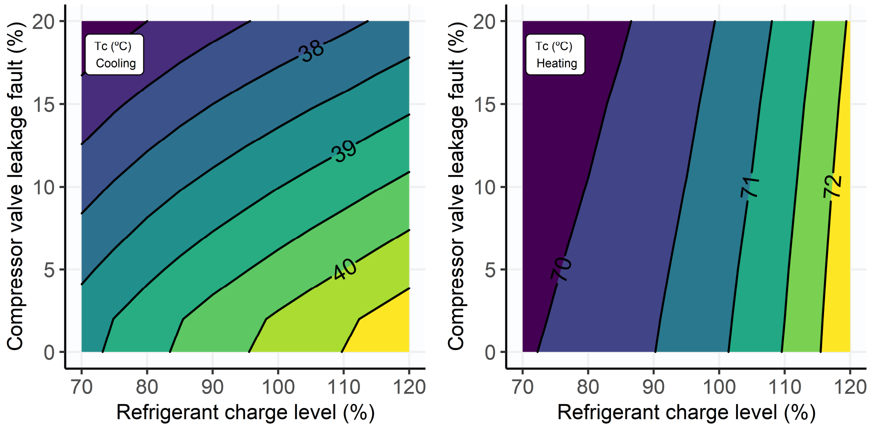

Figure 6: Condenser temperature at different CVL and charge fault levels in cooling (left) and heating mode (right).

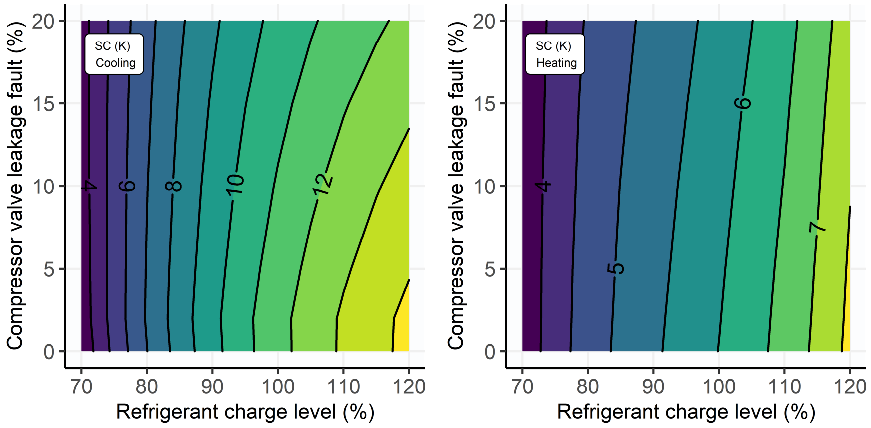

Figure 7: Subcooling at different CVL and charge fault levels in cooling (left) and heating mode (right).

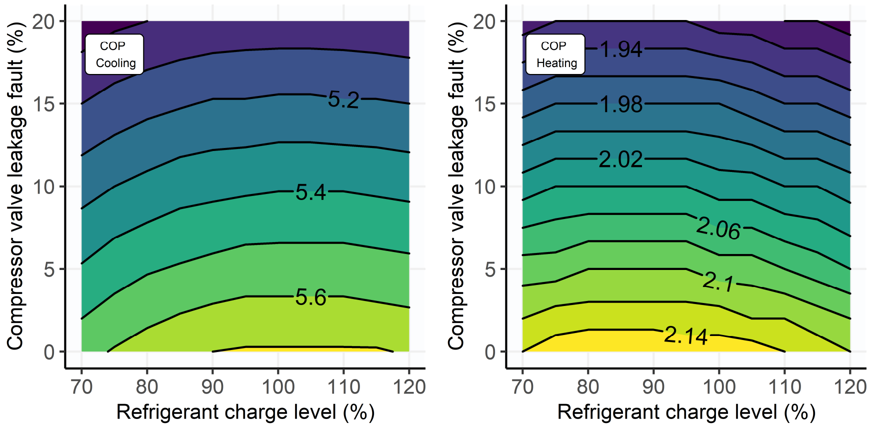

Figure 8: COP at different CVL and charge fault levels in cooling (left) and heating mode (right).

3.4 Simultaneous outdoor unit fouling and refrigerant undercharge/overcharge

This section shows the results for the simultaneous faults of UC/OC and OF. In Figure 9, we show the effects on Tc with these faults. Thus, both OC and OF increase Tc in cooling, but OF to a more significant extent. When both faults coincide in a similar proportion, Tc increases more than if one of the two occurs alone. In the case of UC, the effect on Tc is opposite to that of OF: as the refrigerant charge decreases, Tc decreases. Therefore, if the UC fault occurs when there is OF, we obtain a similar value of Tc as when there is no fault: it reduces the effect of UC on Tc. In heating mode, however, we can see that OF does not affect Tc, as the outdoor unit is the evaporator, and we see here too how the slope changes in the effect of Tc with UC and OC in this mode.

In Figure 10, we can see the effect ts of these simultaneous faults with SC. In cooling mode, when OC and OF increase, SC also increases. OC increases SC more than OF, but the results are similar to if they occurred single in similar proportions. In the case of UC, SC decreases more than OF increases it, so even if they occur at the same time, refrigerant UC can be detected with the decrease of SC. OF does not affect SC in heating mode, so the observed trend is the same as for UC or OC alone if they co-occur.

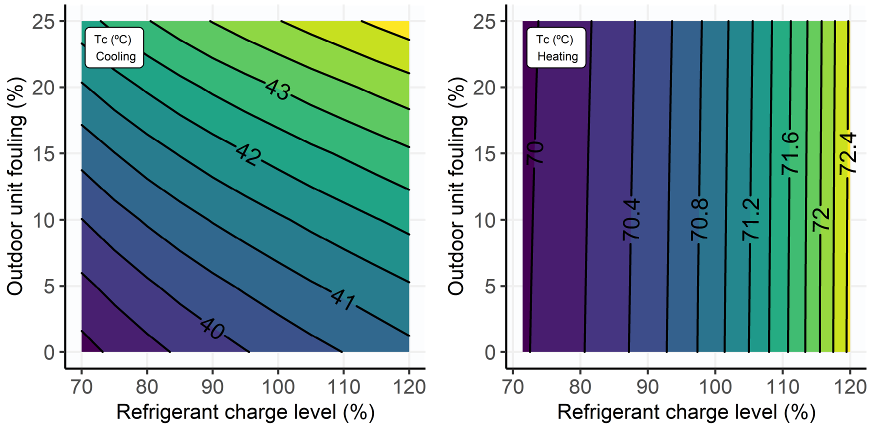

Figure 9: Condenser temperature at different OF and charge fault levels in cooling (left) and heating mode (right).

Figure 11 shows the COP with these faults. Thus, the optimum happens between 90% and 110% of the charge in cooling mode and without OF. If OF and OC occur simultaneously, the latter does not affect so much to worsen the COP with increasing fault level. Nevertheless, in heating mode, the optimum COP is found at lower charge values than at cooling (as seen in the previous section). COP is generally less affected in this mode than in cooling (the maximum variation we see is about 0.05). In addition, OC worsens the COP more.

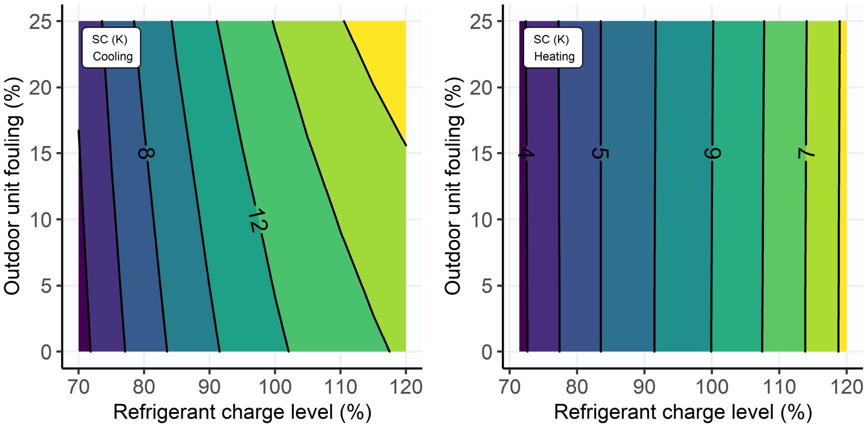

Figure 10: Subcooling at different OF and charge fault levels in cooling (left) and heating mode (right).

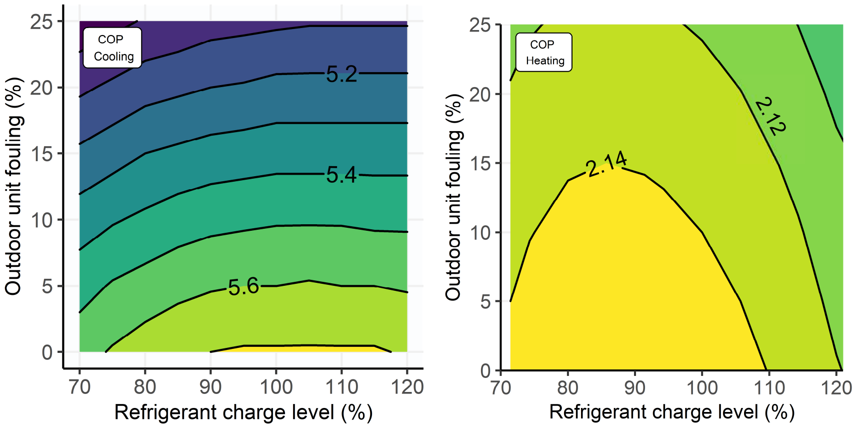

Figure 11: COP at different OF and charge fault levels in cooling (left) and heating mode (right).

3.5 Simultaneous outdoor unit fouling and compressor valve leakage

Figure 12 shows the effects on Tc of simultaneous OF and CVL faults, and Figure 13 shows the effects on SC. Thus, CVL causes both Tc and SC to decrease in cooling mode and OF to increase. Moreover, the slopes with which Tc or SC increase or decrease with fault level are similar. In heating mode, both CVL and OF have little effect on Tc and SC (OF practically none because the outdoor unit is the evaporator), so having these faults simultaneously does not cause significant changes in these variables.

In Figure 14, we can see the COP evolution with these faults. Thus, in cooling, the optimum is found when the fault level of both faults is 0, and it decreases when the fault level of OF or CVL grows. In heating mode, the COP worsens less than in cooling and only by CVL, since OF does not affect.

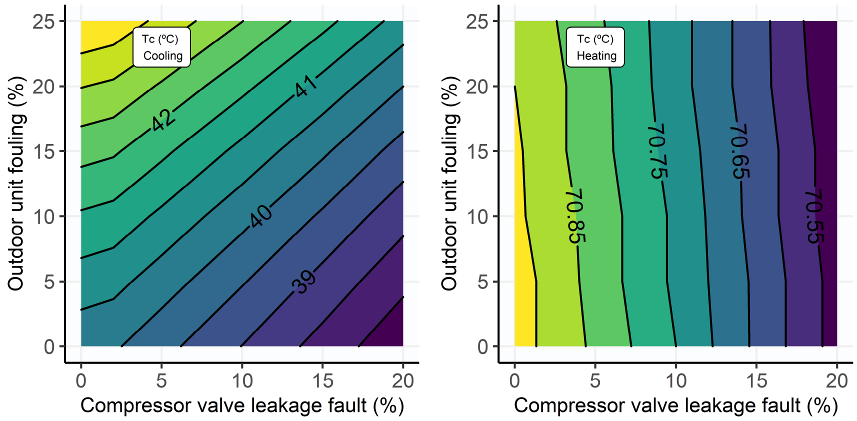

Figure 12: Condenser temperature at different OF and CVL fault levels in cooling (left) and heating mode (right).

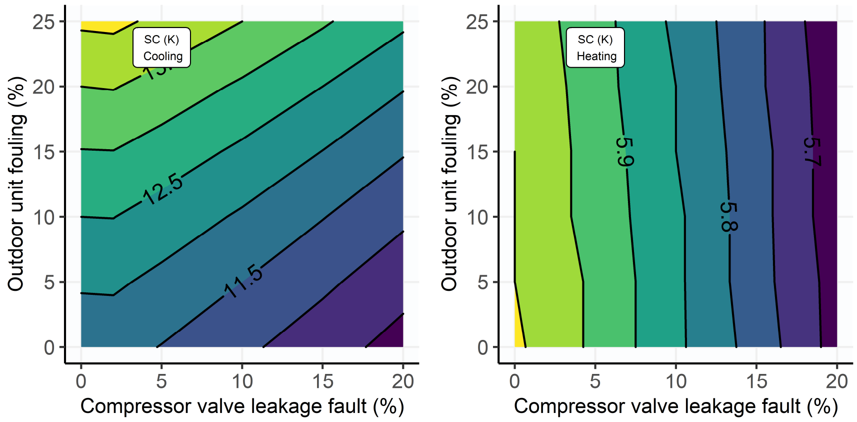

Figure 13: Subcooling at different OF and CVL fault levels in cooling (left) and heating mode (right).

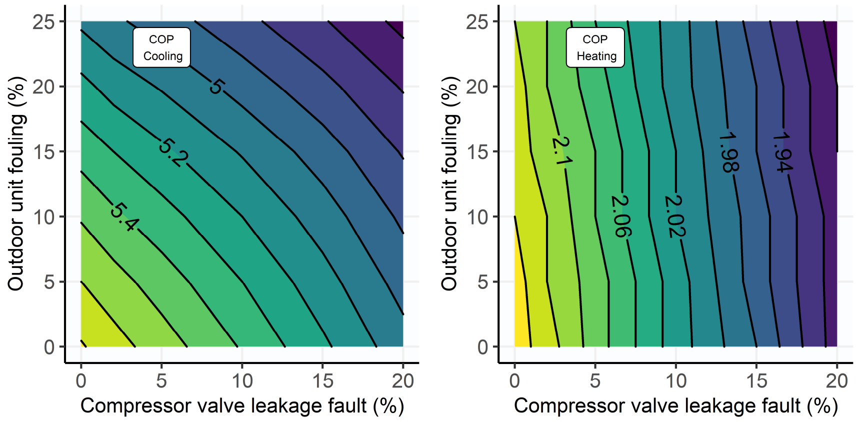

Figure 14: COP at different OF and CVL fault levels in cooling (left) and heating mode (right).

4. CONCLUSIONS

This study has modeled a reversible air-to-water heat pump working with propane. Using this model, some faults have been imposed. The effect of these faults on system variables has been analyzed, intending to be a first step in developing fault detection and diagnosis techniques. Some conclusions drawn from this study are:

- Rules for each operating mode must be designed.

- Cooling mode has shown more sensitivity to faults than heating mode and is more sensitive to cross effect between the three faults analyzed.
- In heating mode, the more relevant effects have been the refrigerant undercharge and overcharge and compressor valve leak.
- Charge faults have shown the lowest effect on the COP of the system unless critical values are presented. Nevertheless, there could be other interests in identifying them as preventing a critical fault or detecting the leak of refrigerants that could be flammable.

NOMENCLATURE

UC	Undercharge	(–)
OC	Overcharge	(–)
CVL	Compressor Valve Leakage	(–)
OF	Outdoor unit fouling	(–)
COP	Coefficient Of Performance	(–)
T	Temperature	(ºC)
SC	Subcooling	(K)
RMSE	Root Mean Square Error	(–)
BPHX	Brazed Plate Heat Exchanger	(–)

Subscript

c	condenser
e	evaporator

REFERENCES

Abbasi, M. H., Abdullah, B., Ahmad, M. W., Rostami, A., & Cullen, J. (2021). Heat transition in the European building sector: Overview of the heat decarbonisation practices through heat pump technology. *Sustainable Energy Technologies and Assessments*, *48*(January), 101630. https://doi.org/10.1016/j.seta.2021.101630

Boahen, S., Mensah, K., Anka, S. K., Lee, K. H., & Choi, J. M. (2021). Fault Detection Algorithm for Multiple-Simultaneous Refrigerant Charge and Secondary Fluid Flow Rate Faults in Heat Pumps. *Energies*, *14*(13), 3877. https://doi.org/10.3390/en14133877

Cheung, H., & Braun, J. E. (2013). Simulation of fault impacts for vapor compression systems by inverse modeling. Part II: System modeling and validation. *HVAC and R Research*, *19*(7), 907–921. https://doi.org/10.1080/10789669.2013.819769

Corberán, J. M., Gonzálvez-Maciá, J., Montes, P., & Blasco, R. (2002). "ART", a computer code to assist the design of refrigeration and air conditioning equipment. *International Refrigeration and Air Conditioning Conference*. http://www.imst-art.com/

European Comission. (2018). *Directive (EU) 2018/844 of the European Parliament and of the Council of 30 May 2018 amending Directive 2010/31/EU on the energy performance of buildings and Directive 2012/27/EU on energy efficiency*.

Hu, Y., & Yuill, D. P. (2021). Effects of multiple simultaneous faults on characteristic fault detection features of a heat pump in cooling mode. *Energy and Buildings*, *251*, 111355. https://doi.org/10.1016/j.enbuild.2021.111355

Kim, M., Payne, W. V., Domanski, P. A., Yoon, S. H., & Hermes, C. J. L. (2006). Performance of a Residential Heat Pump Operating in the Cooling Mode With Single Faults Imposed. In *NIST Publication* (Vol. 29, Issue 4). Elsevier Ltd. https://doi.org/10.1016/j.applthermaleng.2008.04.009

Mehrabi, M., & Yuill, D. (2018). Generalized effects of faults on normalized performance variables of air conditioners and heat pumps. *International Journal of Refrigeration*, *85*, 409–430. https://doi.org/10.1016/j.ijrefrig.2017.10.017

ACKNOWLEDGEMENT

The authors would like to acknowledge the Spanish "Ministerio de Ciencia e Innovación", through the project ref: PID2020-115665RB-I00 "Decarbonización de edificios e industrias con sistemas híbridos de bomba de calor". Belén Llopis-Mengual acknowledges the Spanish "Ministerio de Universidades" through the program ref. FPU 19/04012.